RESEARCH ARTICLE

Computational Predicted Mechanism of Tiliroside Compound Against Triple-Negative Breast Cancer Using Network Pharmacology and Induced-Fit Docking Approach

Tegar Achsendo Yuniarta[1], Dwi Syah Fitra Ramadhan[2,*], Zulfikar Ali Hasan[3], Mansur Mansur[4]

[1]Department of Drug Discovery and Development, Faculty of Pharmacy, Universitas Surabaya, Jl. Tenggilis Mejoyo Blok AM No.12, Surabaya 60293, Indonesia
[2]Department of Pharmacy, Politeknik Kesehatan Kemenkes Makassar, Jl. Wijaya Kusuma Raya No. 46, Makassar 90222, Indonesia
[3]Department of Medical Laboratory and Technology, Politeknik Kesehatan Kemenkes Makassar, Jl. Wijaya Kusuma Raya No. 46, Makassar 90222, Indonesia
[4]Department of Pharmacy, Faculty of Pharmacy, Universitas Megarezky, Jl. Antang Raya No. 43-45, Makassar 90234, Indonesia

*Corresponding author. Email: dwisyahfitra@poltekkes-mks.ac.id

Received date: Jun 30, 2026; Revised date: Aug 3, 2026; Accepted date: Aug 4, 2026

Abstract

BACKGROUND: Triple-negative breast cancer (TNBC) progression is driven by dysregulation of multiple interconnected signaling pathways rather than a single molecular abnormality, but current treatment strategies TNBC primarily rely on single-target therapy, highlighting the need for therapeutic candidates that may target multiple signaling pathway of TBNC. Tiliroside, a naturally occurring flavonoid glycoside, has demonstrated promising anticancer activity; however, its predicted effects on TNBC-associated oncogenic signaling networks remain poorly understood. Therefore, this study aimed to investigate the predicted molecular mechanisms by which tiliroside may modulate TNBC-associated oncogenic signaling networks.

METHODS: Integrated computational approach combining network pharmacology, comparative molecular docking, and induced-fit docking was employed. Potential targets of tiliroside were predicted using SwissTargetPrediction and intersected with TNBC-associated genes retrieved from GeneCards. Protein–protein interaction and KEGG pathway enrichment analyses were performed to identify key molecular targets and signaling pathways. Comparative molecular docking was subsequently conducted using 19 structurally related flavonoids with reported anticancer activities against the identified hub proteins, followed by induced-fit docking to characterize the binding mechanism of tiliroside.

RESULTS: Fifteen overlapping targets were identified between tiliroside and TNBC. Network analysis highlighted Akt serine/threonine kinase 1 (*AKT1*), sarcoma (*SRC*), and epidermal growth factor receptor (*EGFR*) as the principal hub genes, while the KEGG enrichment revealed significant involvement of phosphoinositide 3-kinase (PI3K)–AKT, erythroblastic leukemia viral oncogene B (ErbB), EGFR tyrosine kinase inhibitor resistance, focal adhesion, and vascular endothelial growth factor (VEGF) signaling pathways. Tiliroside consistently exhibited one of the most favorable binding profiles among the evaluated flavonoids, with binding energies of −9.41, −8.62, and −8.25 kcal/mol toward *AKT1*, *SRC*, and *EGFR*, respectively. Induced-fit docking further confirmed stable hydrogen-bond and hydrophobic interactions within the active sites of these proteins.

CONCLUSION: Tiliroside exerts potential anti-TNBC activity through multitarget modulation of interconnected oncogenic signaling pathways, suggesting that tiliroside might be a promising lead compound for TNBC.

KEYWORDS: tiliroside, triple-negative breast cancer, network pharmacology, induced-fit docking

Indones Biomed J. 2026; 18(4): 352-64

Introduction

Breast cancer remains the most frequently diagnosed malignancy among women and a leading cause of cancer-related mortality worldwide.(1-3) Among its molecular subtypes, triple-negative breast cancer (TNBC) accounts for approximately 15–20% of cases. TBNC is characterized by the absence of estrogen receptor (ER), progesterone receptor (PR), and human epidermal growth factor receptor 2 (HER2), resulting in limited targeted therapeutic options and poor clinical outcomes.(4) The aggressive behavior of TNBC is associated with high molecular heterogeneity, rapid development of therapeutic resistance, and metastatic progression, making it one of the most challenging breast cancer subtypes to treat.(5) TNBC progression is driven by the dysregulation of multiple interconnected signaling pathways rather than a single molecular abnormality. Aberrant activation of key signaling proteins, including epidermal growth factor receptor (EGFR), phosphatidylinositol 3-kinase/protein kinase B (PI3K/AKT), sarcoma (SRC) kinase, focal adhesion kinase (FAK), insulin-like growth factor receptor (IGF1R), and hepatocyte growth factor receptor (MET), contributes to tumor proliferation, survival, invasion, angiogenesis, and treatment resistance.(6,7)

Conventional cancer therapies, such as chemotherapy, are generally based on the single-target paradigm, in which one drug is designed to inhibit a specific molecular target. Although this strategy has achieved clinical success in several cancer subtypes, its effectiveness in TNBC remains limited because TNBC is driven by multiple dysregulated signaling pathways and extensive molecular heterogeneity, which contribute to therapeutic resistance and disease progression.(8–10) Therefore, therapeutic strategies capable of simultaneously modulating multiple molecular targets and interconnected signaling pathways might be more appropriate for TNBC management.

Natural products have historically played a pivotal role in anticancer drug discovery due to their structural diversity and broad pharmacological activities.(11,12) Among them, flavonoids have attracted considerable attention because of their ability to regulate multiple biological processes involved in carcinogenesis, including oxidative stress, inflammation, apoptosis, angiogenesis, and metastatic progression.(13–15) Among flavonoids, tiliroside has attracted increasing attention because of its biological and structural characteristics that make it a promising candidate for multitarget drug discovery in complex diseases, such as TNBC.(16) Recent experimental evidence has further highlighted the therapeutic relevance of tiliroside in TNBC. It is reported that tiliroside significantly inhibited TNBC cell proliferation, migration, invasion, and three-dimensional spheroid formation while suppressing tumor growth and prolonging survival in murine xenograft models.(17) Mechanistically, tiliroside has been identified as a novel inhibitor of carbonic anhydrase XII (CA XII), a hypoxia-associated enzyme involved in tumor progression, extracellular acidification, cancer stemness, and adaptation to the tumor microenvironment. In addition, it has been reported to induce apoptosis in TNBC cells through regulation of the E2F1/3–Caspase-3 signaling axis.(3) Despite these promising anticancer potential of tiliroside, most previous studies have focused on the pharmacological effects of tiliroside or individual molecular targets, whereas its systems-level multitarget mechanisms underlying TNBC remain largely unexplored.

Considering the complex and interconnected signaling networks involved in TNBC progression, a systems-level investigation is required to elucidate the broader pharmacological actions of tiliroside. Therefore, the integration of network pharmacology with comparative molecular docking and induced-fit docking provides a novel strategy to identify key therapeutic targets, evaluate the relative binding potential of tiliroside among related flavonoids, and characterize receptor–ligand interactions considering protein flexibility. This study was conducted to elucidate the molecular mechanisms underlying the anti-TNBC activity of tiliroside by integrating network pharmacology, comparative molecular docking, and induced-fit docking analyses. This integrated computational strategy might provide a comprehensive framework for understanding the multitarget mechanisms of tiliroside and identifying promising molecular targets for future experimental validation.

Methods

Chemical Structure Retrieval and Tiliroside Preparation

The chemical structure of tiliroside (Kaempferol 3-O-(6"-O-p-coumaroyl)-β-D-glucopyranoside) was obtained from the Human Metabolome Database (HMDB). Physicochemical properties, molecular formula, molecular weight, canonical SMILES, and InChIKey were collected and verified prior to computational analyses.(18) The canonical SMILES structure was subsequently used as the input for target prediction and molecular docking studies (Table 1).

Table 1. Physiochemical and structural characteristics of tiliroside.

Parameter	Description
Compound Name	Tiliroside
Synonym	Kaempferol 3-O-(6''-O-p-coumaroyl)-β-D-glucopyranoside
Metabolite ID	C00005851
Molecular Formula	$C_{30}H_{26}O_{13}$
Molecular Weight	594,14 g/mol
CAS Number	20316-62-5
InChIKey	InChI=1S/C30H26O13/c31-16-6-1-14(2-7-16)3-10-22(35)40-13-21-24(36)26(38)27(39)30(42-21)43-29-25(37)23-19(34)11-18(33)12-20(23)41-28(29)15-4-8-17(32)9-5-15/h1-12,21,24,26-27,30-34,36,38-39H,13H2/b10-3+/t21-,24-,26-,27-,30+/m1/s1
SMILES	O=C(/C=C/c1ccc(O)cc1)OC[C@H]1O[C@@H](Oc2c(-c3ccc(O)cc3)oc3cc(O)cc(O)c3c2=O)C(O)C(O)[C@@H]1O

Prediction of Tiliroside-Associated Targets

Potential molecular targets of tiliroside were predicted using the SwissTargetPrediction database (http://www.swisstargetprediction.ch).(8) The canonical SMILES notation of tiliroside was submitted to the database, and Homo sapiens was selected as the target organism. No additional probability threshold was applied, and all predicted targets generated by SwissTargetPrediction were retained for subsequent analyses. This approach was adopted to comprehensively capture the potential target profile of tiliroside before intersection with disease-associated genes. All predicted targets generated by the platform were collected and standardized according to their official gene symbols using the UniProt database. Duplicate targets were removed to obtain the final list of unique tiliroside-associated genes.

Identification of TNBC-Related Genes

Disease-associated targets for TNBC were obtained from the GeneCards database (https://www.genecards.org) using "Triple-Negative Breast Cancer" as the search query. GeneCards compiles gene-centered information from multiple biological and biomedical databases, enabling the identification of genes based on their relevance to specific diseases.(19) To improve the specificity of disease-associated targets, only genes with a relevance score >10 were retained. This cut-off was selected to prioritize genes with strong evidence of association with TNBC while minimizing weakly associated targets.(20) The curated target set served as the reference TNBC gene dataset for subsequent target intersection, network construction, and enrichment analyses.

Identification of Common Therapeutic Targets

The intersection between predicted tiliroside targets and TNBC-associated genes was determined using Venny 2.1.0. A Venn diagram was generated to visualize overlapping genes between the two datasets.(10) The intersecting genes were considered potential therapeutic targets through which tiliroside may exert anti-TNBC effects.

Construction of Compound–Target–Disease Network

The common targets shared between tiliroside and TNBC were imported into Cytoscape version 3.10.2 to construct a compound–target–disease interaction network.(21) In this network, tiliroside and TNBC were designated as the primary nodes, whereas the intersecting genes served as intermediary nodes linking the compound to the disease. Topological analysis of the network was subsequently performed to characterize the relationships among the bioactive compound, disease, and candidate therapeutic targets. The resulting interaction network provided a systems-level representation of the multitarget pharmacological profile of tiliroside and served as the basis for subsequent network analyses.

Protein–Protein Interaction (PPI) Network Construction

To investigate the interactions among the overlapping targets, a PPI network was established using the STRING database (version 12.0; https://string-db.org). The analysis was limited to *Homo sapiens*, and protein associations with a confidence score of ≥0.400 (medium confidence) were retained.(22) Unconnected proteins were omitted from the final network to improve visualization and facilitate interpretation of the interaction patterns. The generated

network was subsequently imported into Cytoscape for topological analysis and the identification of key hub proteins.

Identification of Hub Genes

Hub genes were identified using the CytoHubba plugin implemented in Cytoscape version 3.10.2. Three topological algorithms, namely Degree, Closeness Centrality, and Betweenness Centrality, were employed to evaluate the importance of each node within the PPI network. The Degree method identifies genes with the highest number of direct interactions with neighboring proteins. Closeness Centrality measures the average shortest path between a node and all other nodes in the network, reflecting its ability to rapidly influence other proteins. Betweenness Centrality quantifies the frequency with which a node acts as a bridge connecting different network regions.(23) Genes consistently ranked highly across the three algorithms were considered key hub genes and selected for subsequent molecular docking studies.

Kyoto Encyclopedia of Genes and Genomes (KEGG) Pathway Enrichment Analysis

The biological pathways potentially regulated by the shared targets were investigated through KEGG enrichment analysis using ShinyGO version 0.81. The intersecting gene set was mapped to the *Homo sapiens* pathway database, and statistically overrepresented pathways were identified based on a false discovery rate (FDR) below 0.05. Enrichment outcomes were visualized using bubble plots to facilitate interpretation, with bubble size proportional to the number of mapped genes and color gradients indicating the level of statistical significance.(19)

Protein Preparation for Molecular Docking

The three highest-ranked hub proteins, SRC kinase (PDB ID: 2H8H), AKT1 (PDB ID: 3MV5), and EGFR (PDB ID: 1M17), were selected for docking studies. Three-dimensional crystal structures were downloaded from the Protein Data Bank (https://www.rcsb.org).(24) Before molecular docking, the receptor structures were optimized using the Molecular Operating Environment (MOE) (Chemical Computing Group (CCG), Montreal, QC, Canada). Crystallographic water molecules and irrelevant heteroatoms were excluded from the protein structures, whereas the native co-crystallized ligands were retained for docking validation. The receptors were subsequently protonated under physiological conditions, and atomic partial charges were assigned to ensure appropriate electrostatic representation. Structural optimization was then performed using the Amber force field to generate energetically favorable receptor conformations for subsequent comparative and induced-fit docking simulations.

Ligand Preparation

The three-dimensional structure of ligand was generated and optimized using MOE software. Hydrogen atoms were added, protonation states were adjusted, and the structure was energy-minimized using the MMFF94x force field.(25) The optimized ligand structure was subsequently used for docking simulations.

Docking Protocol Validation

To validate the docking protocol, the co-crystallized ligand of each protein structure was extracted and re-docked into its original binding pocket. The docking protocol was considered valid when the root-mean-square deviation (RMSD) value between the experimental and predicted ligand poses was less than 2.0 Å.(26) These native ligands, namely a quinazoline-based SRC inhibitor (PDB: 2H8H), an ATP-competitive AKT1 inhibitor (PDB: 3MV5), and the EGFR inhibitor erlotinib (PDB: 1M17), represent experimentally validated co-crystallized inhibitors and were retained as reference ligands for comparison of binding affinities and interaction profiles with tiliroside and the comparative flavonoids.

Comparative Induced-Fit Docking Simulation

The comparative induced-fit docking was designed to evaluate the binding performance of tiliroside relative to structurally related flavonoids while using the co-crystallized native ligand of each target protein as a structural reference. This approach enabled assessment of whether the unique structural features of tiliroside, including its glycosylated flavonol scaffold and p-coumaroyl moiety, confer favorable binding characteristics compared with closely related flavonoids, while maintaining comparison with an experimentally validated ligand-binding mode. Induced-fit docking was performed using MOE software to account for receptor flexibility during ligand binding.

To further evaluate the relative molecular performance of tiliroside, comparative docking was subsequently conducted using 19 structurally related flavonoids, predominantly flavonols and their glycosylated derivatives. These compounds were selected because they share a similar flavonol scaffold with tiliroside and have been previously reported to possess anticancer activity. Their inclusion enabled assessment of whether the structural

features of tiliroside confer superior or comparable binding characteristics relative to closely related natural flavonoids, thereby providing a structure–activity perspective within the same chemical class rather than comparison with structurally unrelated compounds.(27) Candidate binding conformations were initially generated using the Triangle Matcher placement algorithm and preliminarily evaluated with the London dG scoring function.

The selected receptor–ligand complexes were subsequently refined under induced-fit conditions using the Amber force field, allowing local structural adaptation of the binding site. Electrostatic interactions beyond the cut-off distance were approximated using the reaction field method, whereas the final binding affinities were estimated using the GBVI/WSA dG scoring function.(30) The induced-fit optimization process was performed using a gradient convergence criterion of 0.01 kcal·mol^{-1}·Å^{-1} with a maximum of 250 iterations. Pharmacophore restraints were incorporated using a force constant of 100, while a radius offset of 0.4 Å was applied to improve ligand accommodation within the binding cavity. The final docking pose for each ligand was selected based on the lowest binding energy score and the most favorable interaction profile with key active-site residues.

Results

Identification of Potential Therapeutic Targets of Tiliroside Against TNBC

SwissTargetPrediction identified 85 potential molecular targets associated with tiliroside (Table 2), reflecting the broad pharmacological spectrum commonly observed among flavonoid-derived natural products. GeneCards database mining initially yielded 6,046 genes associated with TNBC. To increase the reliability of downstream analyses, only genes with a relevance score >10 were retained, resulting in a refined set of 152 high-confidence TNBC-associated genes that served as the disease target dataset for subsequent analyses. The intersection analysis identified 15 common genes shared between tiliroside and TNBC, namely matrix metalloproteinase-9 (*MMP9*), prostaglandin-endoperoxide synthase 2 (*PTGS2*), *SRC*, telomerase reverse transcriptase (*TERT*), *EGFR*, ATP-binding cassette subfamily B member 1 (*ABCB1*), *MMP2*, MET proto-oncogene, receptor tyrosine kinase (*MET*), kinase insert domain receptor (*KDR*), *AKT1*, protein tyrosine kinase 2 (*PTK2*), B-Raf proto-oncogene, serine/threonine kinase (*BRAF*), *IGF1R*, estrogen receptor beta (*ESR2*), and phosphatidylinositol-4,5-bisphosphate

Table 2. Predicted target genes of tiliroside identified using SwissTargetPrediction.

Compound Name	Number of Genes	Predicted Target Genes
Tiliroside	100	*CA7, CA4, CA12, CA2, CA9, CA1, CA13, CA14, CA5A, CA6, CBS, AKR1B1, RPS6KA3, RPS6KA1, RPS6KA6, SYNJ2, BACE1, ACHE, KDM1A, NMUR2, MAOA, ADRA2C, ADRA2A, MMP9, MMP13, MMP2, MMP3, XDH, NQO2, P4HB, NOX4, PKM, RNASEL, PTGS2, NAMPT, GUSB, PDE5A, CD38, DPP4, IKBKB, IL2, TNF, ALOX5, ALOX15, ALOX12, PLK1, SRC, TERT, MGAM, PTPN1, HDAC1, HDAC6, ADORA3, MCL1, APP, EGFR, ABCC1, CYP1B1, PPARG, TXNRD1, ABCG2, KCNA3, ABCB1, BCL9, PLG, PYGL, EPHX2, SNCA, ALDH2, ALDH1B1, ALDH1A2, BCHE, MET, PNLIP, TYR, SYK, SOST, CYP19A1, KDR, AKT1, AURKB, PTK2, CSNK2A1, FLT3, BRAF, IGF1R, INSR, SLCO2B1, NUAK1, ESR2, ELANE, PRKCA, PIK3CG, PIK3CA, MKNK2, AHR, PIM1, FTO, PDE4D, SLC5A2.*
TNBC	152	*ERBB2, BRCA1, CD274, EGFR, BRCA2, TP53, MTOR, PIK3CA, ESR1, STAT3, CTNNB1, PTEN, PARP1, PDCD1, BARD1, NFKB1, MYC, HIF1A, PALB2, CDK4, AKT1, H19, GAS5, LINC-ROR, TACSTD2, AR, ESR2, CHEK2, MET, XIST, KRAS, DANCR, CD44, CASP3, MEG3, CDK6, ATM, CCND1, MIR373, BCL2, MUC1, MIR145, CDH1, CHEK1, EZH2, VEGFA, STING1, RAD51, MIR125A, CXCR4, IL6, MMP9, BCAR4, CERNA3, BRAP, NOTCH1, RB1, GATA3, LOC126862571, MRE11, TUG1, GSK3B, BRAF, MIR451A, YAP1, MIR21, AURKA, MMP2, IGF1R, CTLA4, WEE1, BIRC5, LINC01139, FGFR1, PTK2, FOXM1, MDM2, ZEB1, PTGS2, LINC00511, MIR18A, STAT1, LINC01672, MIR155, FANCM, CDK1, LINC00993, CASP8, MKI67, MIR200C, CYTOR, SNAI1, MIR381, FGFR2, HEIH, FOXC1, NRAS, JAK2, MAPK3, CDK12, MAPK1, DNMT1, MIR136, BAX, MIR205, STK11, CCAT1, MIR206, KDR, MIR146B, MIR100HG, MIR17, BRD4, BCYRN1, MIR200B, TERT, MIR655, MDM4, AXL, FOXA1, MLH1, EPCAM, MIR210, LINP1, ZEB2-AS1, MIR128-2, MIR320A, ABCB1, MIRLET7C, C11orf65, ERBB3, FGFR3, RAD51D, MSH2, KIT, LDHA, HOTTIP, SRC, GPR161, MIR9-1, LINC02605, NBN, MSH6, ATR, CDK2, SMARCA4, LINC00673, MANCR, KRT5, TWIST1, PGR, FOXP3.*

3-kinase catalytic subunit alpha (*PIK3CA*) (Figure 1). Additionally, the compound–target–disease network was constructed to visualize the complex interactions among tiliroside, TNBC, and their associated molecular targets (Figure 2). The network topology highlights the multi-target pharmacological nature of tiliroside against TNBC.

KEGG enrichment analysis revealed that the common targets were significantly involved in multiple cancer-related pathways, including endocrine resistance, EGFR tyrosine kinase inhibitor resistance, proteoglycans in cancer, focal adhesion, VEGF signaling pathway, ErbB signaling pathway, and estrogen signaling pathway (Figure 3). These pathways are closely associated with tumor proliferation, angiogenesis, metastasis, cell survival, and drug resistance. Among these pathways, EGFR tyrosine kinase inhibitor resistance and ErbB signaling are particularly relevant to TNBC because EGFR overexpression is frequently observed in this breast cancer subtype. Furthermore, enrichment of focal adhesion and VEGF signaling pathways suggests that tiliroside may interfere with cell migration, invasion, and tumor angiogenesis. The simultaneous enrichment of multiple pathways supports the hypothesis that tiliroside exerts a multi-target therapeutic effect rather than acting through a single molecular mechanism.

Hub Gene Identification

After PPI network analysis using Degree, Closeness Centrality, and Betweenness Centrality, all three methods consistently identified *SRC*, *AKT1*, and *EGFR* as the highest-ranked hub genes (Table 3), indicating that these proteins occupy central regulatory positions within the TNBC interaction network. High Degree and Closeness Centrality values reflect extensive molecular connectivity and efficient communication with other network components, whereas high Betweenness Centrality indicates an important role in linking multiple signaling modules. Their consistent prioritization therefore supports their selection as representative targets for subsequent molecular docking analyses.

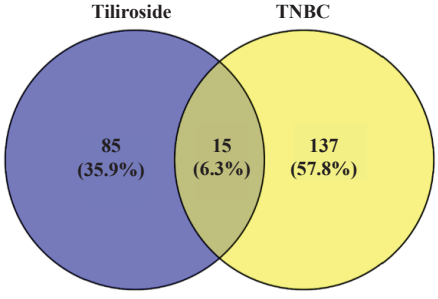

Figure 1. Venn diagram illustrating the overlap between predicted targets of tiliroside and TNBC-related genes.

Among the identified hub genes, *SRC*, *AKT1*, and *EGFR* are key oncogenic regulators that play important roles in TNBC progression, although these signaling proteins are also implicated in multiple other cancer types. SRC functions as a non-receptor tyrosine kinase that integrates signals from multiple receptor tyrosine kinases and promotes proliferation, invasion, epithelial–mesenchymal transition, metastasis, and therapeutic resistance. *AKT1* is a central component of the PI3K/AKT pathway that regulates cell survival, proliferation, metabolism, angiogenesis, and apoptosis resistance, whereas *EGFR* activates multiple downstream signaling cascades, including PI3K/AKT, RAS/MAPK, and *SRC* pathways, thereby enhancing tumor growth and metastatic potential. The close functional relationship among these proteins suggests that simultaneous modulation of *SRC*, *AKT1*, and *EGFR* may provide greater therapeutic benefit than inhibition of a single target.

Several additional hub proteins, including KDR, MET, IGF1R, PIK3CA, PTK2, MMP2, MMP9, PTGS2, and BRAF, further support the complex molecular landscape of TNBC. These proteins regulate complementary biological processes such as angiogenesis, extracellular matrix remodeling, inflammation, focal adhesion, and receptor tyrosine kinase signaling. Their extensive cross-talk with *SRC*, *AKT1*, and *EGFR* contributes to the molecular heterogeneity and adaptive therapeutic resistance characteristic of TNBC, highlighting the importance of multitarget therapeutic strategies.

The hub gene profile was highly consistent with the KEGG enrichment results, which highlighted the PI3K–AKT, ErbB, EGFR tyrosine kinase inhibitor resistance, focal adhesion, and VEGF signaling pathways. Collectively, these findings suggest that the potential anti-TNBC activity of tiliroside may involve coordinated modulation of TNBC-associated oncogenic signaling networks, rather than selective inhibition of a single protein. The identification of *SRC*, *AKT1*, and *EGFR* as the principal hub genes therefore provides a strong biological rationale for the subsequent comparative molecular docking and induced-fit docking analyses.

Induced-Fit Docking Analysis

Based on the network pharmacology results, *SRC*, *AKT1*, and *EGFR* were selected for induced-fit docking to validate the predicted targets and investigate the binding mechanism of tiliroside. Prior to docking, the protocol was validated by

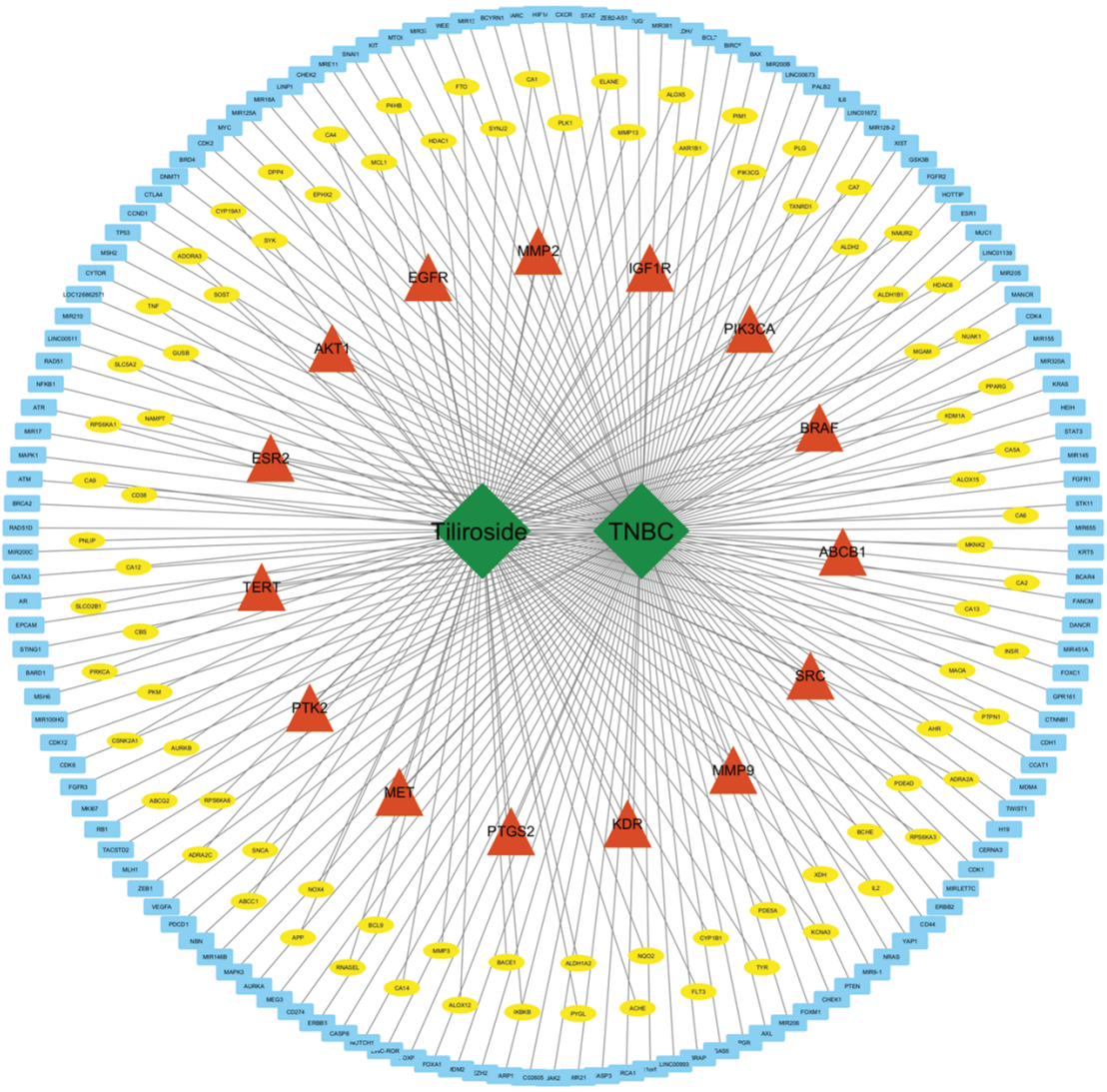

Figure 2. Compound-target-disease network diagram illustrating the intersection between Tiliroside and TNBC. The green diamond nodes represent the compound and the disease. Red triangular nodes denote the shared overlapping therapeutic targets between Tiliroside and TNBC. Yellow elliptical nodes represent the specific target genes unique to Tiliroside, while light blue rectangular nodes represent the target genes associated with TNBC pathogenesis.

redocking the co-crystallized ligands into their respective binding sites (Figure 4). The obtained RMSD values were 1.19 Å for SRC (2H8H), 0.68 Å for AKT1 (3MV5), and 1.06 Å for EGFR (1M17), all below the accepted threshold of 2.0 Å, confirming the reliability of the docking protocol for reproducing the experimental ligand conformations.

To provide a comparative assessment, molecular docking was performed against the three hub proteins using 19 structurally related flavonol-derived compounds with reported anticancer activities (Table 4). The evaluated compounds included astragalin, casticin, dihydromyricetin, fisetin, galangin, gnetin C, hyperoside, isoquercetin, isorhamnetin, kaempferide, kaempferol, kumatakenin, myricetin 3-O-rutinoside, narcissin, nicotiflorin, quercetin, quercitrin, rutin, and tiliroside. These flavonoids were selected because they share structural similarity with tiliroside and have been widely reported to exhibit anticancer activities through modulation of multiple oncogenic pathways. Tiliroside consistently ranked among the best-performing compounds, exhibiting the strongest binding affinity toward AKT1 (−9.41 kcal/mol), a binding affinity comparable to the native ligand for SRC (−8.62 kcal/mol), and the second strongest affinity toward EGFR (−8.25 kcal/mol), surpassed only by myricetin 3-O-rutinoside. These findings support the selection of tiliroside for detailed interaction analysis.

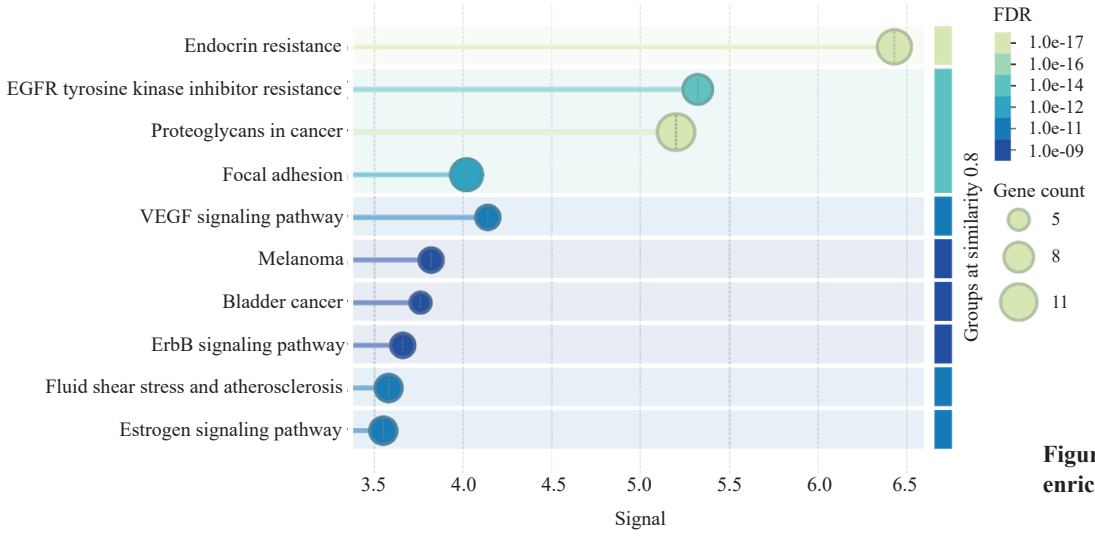

Figure 3. KEGG pathways enrichment analysis.

The interaction profiles of tiliroside with the three hub proteins were summarized in Table 5 and Figure 5. Within the SRC kinase domain, the native ligand formed the characteristic hinge-region hydrogen bond with Met341, whereas tiliroside adopted an alternative binding mode through hydrogen bonding with Phe405 while maintaining extensive hydrophobic interactions with residues surrounding the ATP-binding pocket. This interaction pattern produced a binding affinity comparable to that of the native inhibitor, indicating that tiliroside might be effectively accommodated within the SRC catalytic cavity.

Table 3. Top hub genes identified from protein–protein interaction network based on degree, closeness, and betweenness centrality analyses.

Gene	Degree Score	Closeness Score	Betweenness Score
SRC	14	14.0	4.955.556
AKT1	14	14.0	4.955.556
EGFR	14	14.0	4.955.556
KDR	13	13.5	3.642.063
MMP9	13	13.5	3.997.619
IGF1R	12	13.0	1.880.159
MET	12	13.0	2.858.730
MMP2	12	13.0	2.235.714
PTGS2	11	12.5	–
PTK2	10	12.0	–
PIK3CA	–	–	2.418.254
BRAF	–	–	1.815.079

Among the investigated targets, *AKT1* exhibited the strongest interaction with tiliroside. Unlike the native ligand, which interacted with the hinge residues Glu228 and Ala230, tiliroside established hydrogen bonds with Lys179 and Asp439 while forming extensive hydrophobic contacts throughout the binding pocket. These interactions resulted in a substantially lower docking score (−9.41 kcal/mol) than the native ligand (−7.07 kcal/mol), suggesting highly favorable binding within the AKT1 kinase domain and supporting *AKT1* as a major molecular target of tiliroside.

A similar interaction pattern was observed for *EGFR*. Although tiliroside did not reproduce the canonical hinge interaction of the native ligand, it formed stable hydrogen bonds with Lys721 and Asp831 together with a π–H interaction involving Phe699 and multiple hydrophobic contacts within the catalytic pocket. These interactions generated a stronger binding affinity (−8.25 kcal/mol) than the native ligand (−7.71 kcal/mol), indicating favorable accommodation of tiliroside within the *EGFR* active site.

Overall, the current docking results demonstrate that tiliroside does not strictly mimic the binding mode of the co-crystallized inhibitors but instead adopts a flexible interaction strategy combining alternative hydrogen bonds with extensive hydrophobic contacts. Its consistently favorable binding affinities across *SRC*, *AKT1*, and *EGFR*, together with the comparative docking results against 19 structurally related flavonoids, support the hypothesis that tiliroside functions as a multitarget kinase modulator. These structural findings are in good agreement with the network pharmacology analysis, which identified the same proteins as the principal hub genes involved in TNBC-associated signaling pathways.

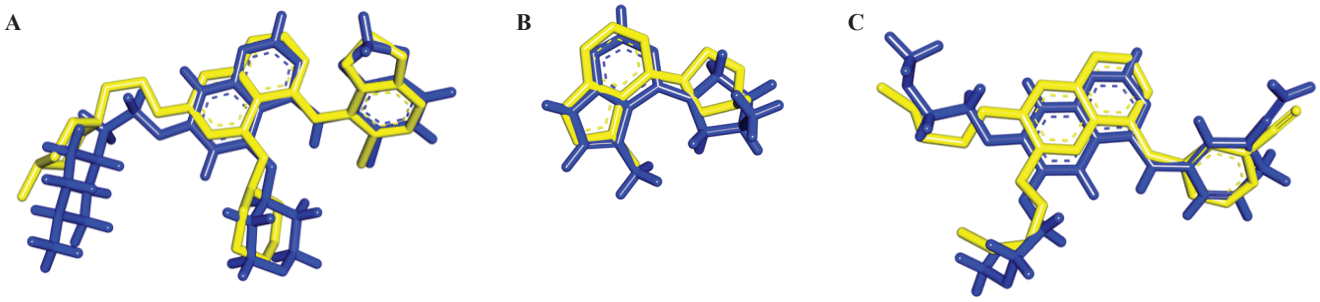

Figure 4. docking validation of the three potential principal hub proteins. A: SRC kinase (2H8H); B: AKT1 (3MV5); C: EGFR (1M17). The rmsd value 1.19 Å, 0.68 Å, and 1.06 Å, respectively.

Discussion

The identification of 15 overlapping targets suggests that the computationally predicted anticancer activity of tiliroside may involve coordinated modulation of multiple oncogenic proteins rather than selective inhibition of a single molecular target. Such a multitarget profile is particularly relevant for TNBC, a highly heterogeneous malignancy in which extensive cross-talk among proliferative, metastatic, inflammatory, and survival pathways contributes to therapeutic resistance and disease progression.(28–32) This systems-level prediction is consistent with the growing recognition that natural flavonoids exert their pharmacological activities through simultaneous regulation of interconnected signaling networks instead of the conventional one-drug–one-target paradigm. Studies have also demonstrated that tiliroside suppresses cancer cell proliferation, migration, and inflammatory responses through modulation of multiple signaling pathways in different cancer models, supporting the plausibility of the multitarget interactions predicted in the present computational analysis.(32–34)

Table 4. Comparative molecular docking results of tiliroside, structurally related flavonoids with reported anticancer activity, and native ligands against the three principal hub proteins (SRC kinase, AKT1, and EGFR) identified from network pharmacology analysis.

Name	Binding Energy (kcal/mol)		
	SRC Kinase (2H8H)	AKT-1 (3MV5)	EGFR (1M17)
Native Ligand	-8.63	-7.07	-7.71
Astragalin	-7.28	-7.71	-7.22
Casticin	-7.11	-7.9	-6.76
Dihydromyricetin	-6.56	-6.63	-6.34
Fisetin	-6.24	-6.18	-6.06
Galangin	-5.96	-5.78	-5.91
GnetinC	-6.26	-6.65	-6.95
Hyperoside	-7.13	-7.66	-7.14
Isoquercetin	-6.89	-8.21	-7.3
Isorhamnetin	-6.79	-6.74	-6.17
Kaempferide	-6.49	-6.52	-6.07
Kaempferol	-6.24	-6.01	-6.11
Kumatakenin	-6.22	-6.77	-6.34
Myricetin 3-O-rutinoside	-8.18	-8.52	-8.47
Narcissin	-7.72	-8.09	-7.89
Nicotiflorin	-8.35	-7.89	-7.72
Quercetin	-6.45	-6.38	-6.24
Quercitrin	-7.35	-7.4	-6.78
Rutin	-7.46	-8.28	-8.24
Tiliroside	-8.62	-9.41	-8.25

Binding affinities are expressed as docking scores (kcal/mol), where more negative values indicate stronger predicted protein–ligand interactions.

Table 5. Integrated molecular docking scores and interaction profiles of native ligands and tiliroside across SRC (2H8H), AKT1 (3MV5), and EGFR (1M17) kinase domains.

Receptor (PDB ID)	Ligand	Binding Energy (kcal/mol)	Key Hydrogen Bond/ Polar Anchors	π-System/ Electrostatic Interactions	Hydrophobic Contacts
SRC Kinase (2H8H)	Native	-8.63	Met341 *(backbone)*	Solvent exposure at cationic piperazine ring	Leu273, Val281, Ala293, Ile294, Ile336, Ala390, Leu393, Ala403
	Tiliroside	-8.49	Phe405 *(backbone)*	Polar stabilization surrounding the glucopyranoside core	Leu273, Val281, Ala293, Ile294, Met314, Val323, Leu325, Ile336, Leu347, Ala390, Leu393, Ala403
AKT1 (3MV5)	Native	-7.07	Glu228, Ala230 *(hinge)*	Glu224, Met231, Asp292 *(Salt bridge/Ion pair)*	Leu159, Val164, Ala177, Met227, Ala230, Met231, Phe408
	Tiliroside	-9.41	Lys179 *(sidechain)* , Asp439 (sidechain)	Hydrophilic carbohydrate scaffold extending into the solvent phase	Leu156, Phe161, Val164, Ile180, Leu181, Met281, Phe237, Phe438, Phe442
EGFR (1M17)	Native	-7.71	Met769 *(hinge backbone)*	Solvent exposure at extended methoxyethoxy chains	Leu694, Val702, Ala719, Ile720, Leu764, Ile765, Leu768, Pro770, Leu820
	Tiliroside	-8.25	Lys721 *(sidechain)* , Asp831 (carboxylate)	Phe699 *(π-H interaction)*	Leu694, Val702, Ala719, Leu764, Leu768, Pro770, Phe771, Leu820

The pathway enrichment results further reinforce this multitarget hypothesis by indicating that the predicted targets are involved in interconnected oncogenic signaling networks governing cell proliferation, apoptosis resistance, angiogenesis, migration, and therapeutic resistance. Rather than acting through a single pathway, tiliroside may influence several complementary signaling cascades, including PI3K/AKT, ErbB, EGFR tyrosine kinase inhibitor resistance, focal adhesion, and VEGF signaling pathways. Such coordinated regulation may be advantageous in TNBC, where compensatory activation of alternative pathways frequently limits the long-term efficacy of conventional single-target therapies.(33) Among the predicted targets, SRC, AKT1, and EGFR emerged as central regulatory nodes within the TNBC-associated protein interaction network, suggesting that these proteins may play key roles in mediating the multitarget activity of tiliroside. Rather than indicating disease-specific biomarkers, their central positions highlight their importance in integrating multiple signaling pathways associated with tumor growth, survival, invasion, and therapeutic resistance.(35)

While the structurally related flavonoids enabled evaluation of the relative binding performance of tiliroside within the flavonol subclass, the native ligands provided experimentally validated reference binding modes for SRC, AKT1, and EGFR. Compared with the evaluated flavonoids, tiliroside consistently exhibited one of the most favorable binding profiles across all three targets, showing the strongest predicted affinity toward AKT1, binding affinity comparable to the native inhibitor for SRC, and one of the highest affinities toward EGFR. These observations suggest that the molecular architecture of tiliroside, consisting of a kaempferol backbone linked to a glucosyl moiety and a p-coumaroyl group, provides structural features that favor complementary hydrogen-bonding and hydrophobic interactions within kinase binding pockets. (17) The glucose moiety contributes multiple hydrogen-bond donors and acceptors, whereas the aromatic flavonol and p-coumaroyl groups facilitate extensive hydrophobic and π-mediated interactions, potentially explaining that the favorable interaction profiles might predict across multiple kinase targets.(12)

The induced-fit docking further strengthened these predictions by incorporating receptor flexibility during ligand binding. Although tiliroside adopted binding conformations distinct from those of the co-crystallized inhibitors, it maintained stable hydrogen-bond and hydrophobic interaction networks across SRC, AKT1, and EGFR, supporting the computational hypothesis that the compound possesses sufficient conformational

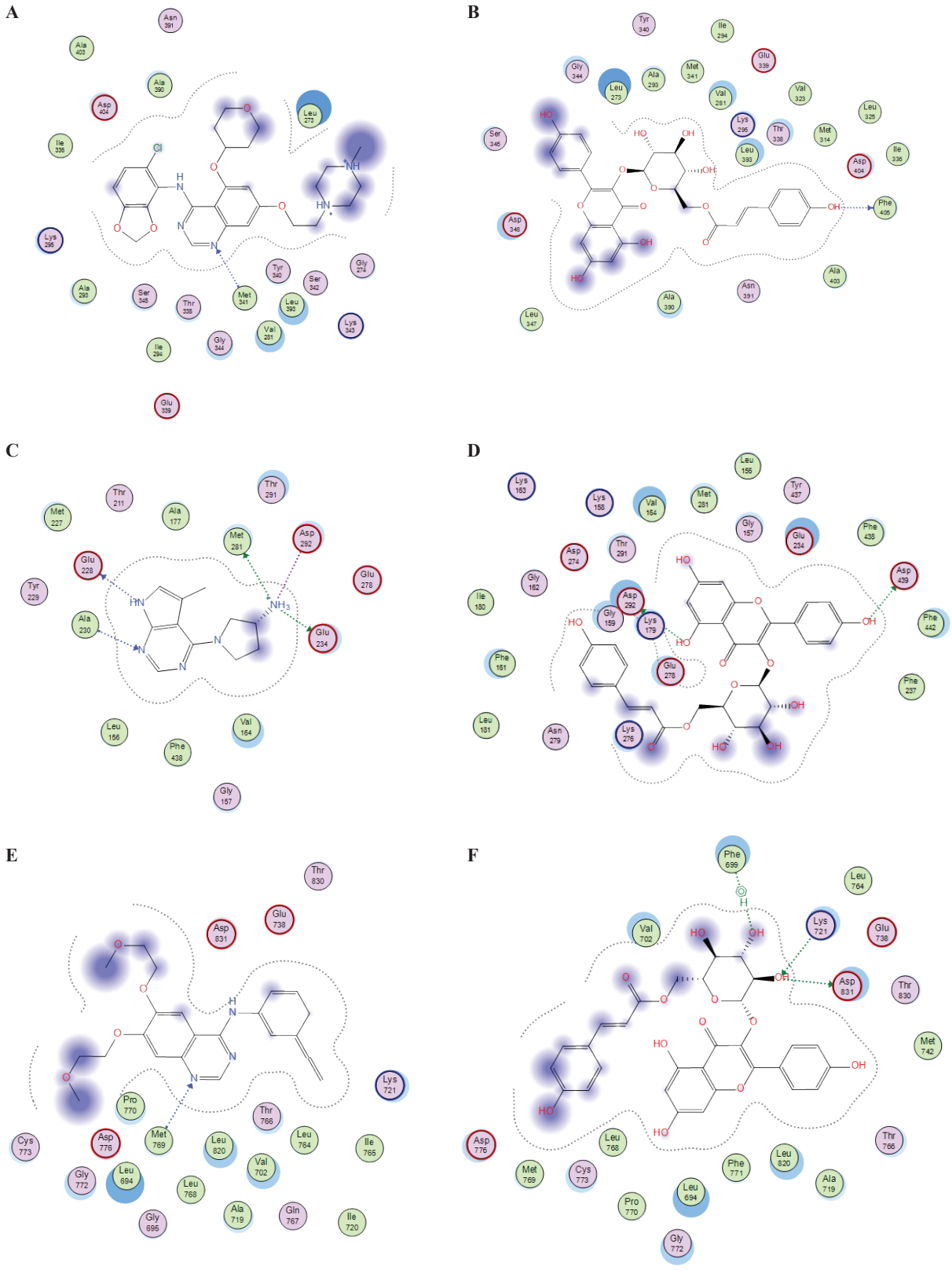

Figure 5. 2D interaction diagram of native ligands and tiliroside across SRC (2H8H), AKT1 (3MV5), and EGFR (1M17) kinase domains. A: SRC (2H8H), native; B: SRC (2H8H), tiliroside; C: AKT1 (3MV5), native; D: AKT1 (3MV5), tiliroside; E: EGFR (1M17), native; F: EGFR (1M17), tiliroside. The diagram illustrates the interaction types and properties between the ligand and receptor. Residue types are color-coded as polar (purple), acidic (red outline), basic (blue outline), and greasy (green). Hydrogen bonding and backbone interactions are represented by directional dashed arrows: green for sidechain acceptor/donor and blue for backbone acceptor/donor. Solvent and metal environments are denoted by solvent residues (white circles), metal complexes (grey circles), solvent contacts (yellow dotted lines), and metal/ion contacts (purple dotted lines). Lastly, structural boundaries and exposure levels are delineated by the proximity contour (dashed cloud), ligand exposure (blue blur), and receptor exposure (blue/white crescent).

adaptability to interact with structurally distinct kinase targets.

Overall, the present computational findings suggest that tiliroside may exert anticancer activity through coordinated modulation of multiple oncogenic signaling pathways associated with TNBC progression. This study provides a systems-level computational framework that generates testable hypotheses regarding the multitarget pharmacological potential of tiliroside. Nevertheless, these findings are based on computational analyses, including target prediction, network pharmacology, and induced-fit molecular docking, which depend on available databases and do not fully capture the dynamic complexity of protein–ligand interactions under physiological conditions. Therefore, further validation through molecular dynamics simulations and experimental studies is warranted to confirm the predicted target interactions and clarify the therapeutic potential of tiliroside in TNBC.

Conclusion

Tiliroside exerts potential anti-TNBC activity through multitarget modulation of interconnected oncogenic signaling pathways, with SRC, AKT1, and EGFR emerging as the principal hub proteins within the TNBC-associated interaction network. Even after comparative docking against 19 structurally related flavonoids, together with comparison to the co-crystallized native ligands, tiliroside exhibited one of the most favorable predicted binding profiles. These computational findings suggest that tiliroside may represent a promising multitarget flavonoid with the potential to modulate oncogenic signaling pathways associated with TNBC progression.

Acknowledgments

The authors would like to thank the Politeknik Kesehatan Kemenkes Makassar for providing academic support and research facilities. We also sincerely appreciate to Institute Teknologi Bandung for supporting this study, particularly through the provision of specialized research software that enabled the completion of the computational analyses.

Authors Contribution

TAY contributed to the study design, supervised the research, interpreted the results, and critically revised the manuscript. DSFR conceived and designed the study, performed the network pharmacology, comparative molecular docking, and induced-fit docking analyses, interpreted the data, prepared the figures and tables, and drafted the manuscript. ZAH participated in data analysis, validated the computational workflow, and contributed to manuscript revision. MM assisted in data interpretation, reviewed the manuscript for important intellectual content, and approved the final version for publication. All authors read and approved the final manuscript and agree to be accountable for all aspects of the work.

Ethical Statement

Ethical approval and informed consent were not required for this work.

Conflict of Interest

Authors declare no conflict of interest.

References

1. Bray F, Laversanne M, Sung H, Ferlay J, Siegel RL, Soerjomataram I, *et al.* Global cancer statistics 2022: GLOBOCAN estimates of incidence and mortality worldwide for 36 cancers in 185 countries. CA Cancer J Clin. 2024; 74(3): 229–63.
2. Abdihalim TS, Idris AAA. Mucin level as a potential biomarker for breast cancer diagnosis. Mol Cell Biomed Sci. 2022; 6(3): 117–20.
3. Widowati W, Jasaputra DK, Sumitro SB, Widodo MA, Afifah E, Rizal R, *et al.* Direct and indirect effect of TNFα and IFNγ toward apoptosis in breast cancer cells. Mol Cell Biomed Sci. 2018; 2(2): 60–9.
4. Agelidis A, Ter-Zakarian A, Jaloudi M. Triple-negative breast cancer on the rise: breakthroughs and beyond. Breast Cancer. 2025; 17: 523–9.
5. Sood D, Kaur C, Kumar N, Kumar R, Singh G. Triple-negative breast cancer: Challenges, advances, and promising therapeutic interventions. Med Oncol. 2025; 42(11): 506. doi: 10.1007/s12032-025-03066-9.
6. Li Y, Zhang H, Merkher Y, Chen L, Liu N, Leonov S, *et al.* Recent advances in therapeutic strategies for triple-negative breast cancer. J Hematol Oncol. 2022; 15(1): 121. doi: 10.1186/s13045-022-01341-0.
7. Dewi C, Fristiohady A, Amalia R, Khairul Ikram NK, Ibrahim S, Muchtaridi M. Signaling pathways and natural compounds in triple-negative breast cancer cell line. Molecules. 2022; 27(12): 3661. doi: 10.3390/molecules27123661.
8. Umar AH, Biringallo CSN, Tuyuwale PI, Kila A, Febyola KD, Syahruni R, *et al.* Unveiling the pharmacological mechanism of Cosmos caudatus compounds as lung cancer drug candidates:

Pharmacology networking, molecular docking, and experimental Validation. J Pharm Innov. 2025; 20(3): 81. doi: 10.1007/s12247-025-09989-0.

9. Singh T, Rastogi M, Thakur K. Network pharmacology and in silico approach to study the mechanism of quercetin against breast cancer. silico Pharmacol. 2025; 13(1): 22. doi: 10.1007/s40203-025-00306-8.
10. Zheng M, Zhang R, Yang X, Wang F, Guo X, Li L, *et al.* Integrating network pharmacology, molecular docking, and bioinformatics to explore the mechanism of sparganii rhizoma in the treatment of laryngeal cancer. Mol Divers. 2025; 29(6): 6325–42.
11. Ullah A, Munir S, Badshah SL, Khan N, Ghani L, Poulson BG, *et al.* Important flavonoids and their role as a therapeutic agent. Molecules. 2020; 25(22): 5243. doi: 10.3390/molecules25225243.
12. Rusli R, Ramadhan DSF, Rusdiaman R, Fakih TM. Evaluating quercetin analogs from Indonesian bioflavonoids for breast cancer: Insights from in silico and cytotoxicity assays. J Herb Med Pharmacol. 2025; 14(4): 417–25.
13. Aliffia D, Ramadhani DA, Wasityastuti W, Sari DRT, Kustiati U, Wihadmadyatami H, *et al.* Ocimum sanctum leaves prevent neuronal cell apoptosis through reduction of Caspase-3 and -9 expressions and inhibition of β-amyloid oligomerization. Indones Biomed J. 2023; 15(4): 322–32.
14. Ikawati M, Utomo RY, Hapsari NP, Meiyanto E, Oka C. Diosmin enhances the anti-migration activity of curcumin Analog PGV-1 on colorectal cancer cells. Indones Biomed J. 2024; 16(1): 56–65.
15. Yoong WT, Choong SS, Fauzee MSO, Ahmad Z, Hakim MN. Luteolin suppresses endothelial permeability and nitric oxide scavenging effects. Indones Biomed J. 2024; 16(5): 427–33.
16. Luhata LP, Luhata WG. TILIROSIDE: Biosynthesis, bioactivity and structure activity relationship (SAR) - A Review. J Phytopharm. 2017; 6(6): 343–8.
17. Han R, Yang H, Ling C, Lu L. Tiliroside suppresses triple-negative breast cancer as a multifunctional CAXII inhibitor. Cancer Cell Int. 2022; 22(1): 368. doi: 10.1186/s12935-022-02786-6.
18. Kim S, Thiessen PA, Bolton EE, Chen J, Fu G, Gindulyte A, *et al.* PubChem substance and compound databases. 2016; 44: 1202–13.
19. Yu X, Qin W, Cai H, Ren C, Huang S, Lin X, *et al.* Analyzing the molecular mechanism of xuefuzhuyu decoction in the treatment of pulmonary hypertension with network pharmacology and bioinformatics and verifying molecular docking. Comput Biol Med. 2024; 169: 107863. doi: 10.1016/j.compbiomed.2023.107863.
20. Cheng F, Shi Y, Gao X, Han J, Xu B, Cheng X, *et al.* Machine learning-based prognostic model of stemness and angiogenesis-related genes for predicting prognosis and immune infiltration in patients with HCC. Sci Rep. 2026; 16(1): 7271. doi: 10.1038/s41598-026-38379-w.
21. Meinita MDN, Riyanti, Sanjayasari D, Riviani, Harwanto D, Jiso A, *et al.* Bioactive compound profiling of agarophyte seaweed (Gelidiella acerosa, Gracilaria arcuata, and Gracilaria verrucosa) based on LC-HRMS metabolomic and molecular networking approach. Foods. 2025; 14(23): 4042. doi: 10.3390/foods14234042.
22. Szklarczyk D, Nastou K, Koutrouli M, Kirsch R, Mehryary F, Hachilif R*, et al*. The STRING database in 2025: Protein networks with directionality of regulation. Nucleic Acids Res. 2025; 53(D1): D730–7.
23. Che S, Zhou N, Liu Y, Xie J, Liu E. Andrographolide exerts anti-respiratory syncytial virus activity by up-regulating heme oxygenase-1 independent of interferon responses in human airway epithelial cells. Mol Biol Rep. 2023; 50(5): 4261–72.
24. Burley SK, Berman HM, Bhikadiya C, Bi C, Chen L, Di Costanzo L, *et al.* RCSB Protein Data Bank: biological macromolecular structures enabling research and education in fundamental biology, biomedicine, biotechnology and energy. Nucleic Acids Res. 2019; 47(D1): D464–74.
25. Tosco P, Stiefl N, Landrum G. Bringing the MMFF force field to the RDKit: Implementation and validation. J Cheminform. 2014; 6(1): 4–7.
26. Nurisyah, Ramadhan DSF, Dewi R, Asikin A, Daswi DR, Adam A, *et al.* Targeting EGFR allosteric site with marine-natural products of Clathria Sp.: A computational approach. Curr Res Struct Biol. 2024; 7: 100125. doi: 10.1016/j.crstbi.2024.100125.
27. Ramadhan DSF. An integrated machine learning model and induced-fit docking for identifying EGFR inhibitors from marine natural products. Adv Theory Simulations. 2026; 9(3): e70371. doi: 10.1002/adts.70371.
28. Sabbah DA, Hajjo R, Sweidan K. Review on epidermal growth factor receptor (EGFR) structure, signaling pathways, interactions, and recent updates of EGFR inhibitors. Curr Top Med Chem. 2020; 20(10): 815–34.
29. Freitas JT, Jozic I, Bedogni B. Wound healing assay for melanoma cell migration. Methods Mol Biol. 2021; 2265: 65–71.
30. Kopustinskiene DM, Jakstas V, Savickas A, Bernatoniene J. Flavonoids as anticancer agents. Nutrients. 2020; 12(2): 457. doi: 10.3390/nu12020457.
31. Ali N, Akbar R, Saleem A, Ali A, Ali A. AI based natural inhibitor targeting RPS20 for colorectal cancer treatment using integrated computational approaches. Sci Rep. 2025; 15(1): 24906. doi: 10.1038/s41598-025-07574-6.
32. Madera S, Izzo F, Chervo MF, Dupont A, Chiauzzi VA, Bruni S, *et al.* Halting ErbB-2 isoforms retrograde transport to the nucleus as a new theragnostic approach for triple-negative breast cancer. Cell Death Dis. 2022; 13(5): 447. doi: 10.1038/s41419-022-04855-0.
33. Unterleuthner D, Neuhold P, Schwarz K, Janker L, Neuditschko B, Nivarthi H, *et al.* Cancer-associated fibroblast-derived WNT2 increases tumor angiogenesis in colon cancer. Angiogenesis. 2020; 23(2): 159–77.
34. Farhan M, Rizvi A, Aatif M, Ahmad A. Current understanding of flavonoids in cancer therapy and prevention. Metabolites. 2023; 13(4): 481. doi: 10.3390/metabo13040481.
35. Asleh K, Riaz N, Nielsen TO. Heterogeneity of triple negative breast cancer: Current advances in subtyping and treatment implications. J Exp Clin Cancer Res. 2022; 41(1): 265. doi: 10.1186/s13046-022-02476-1.